How to Win the Uncertainty of Ex-vessel Corium Coolability in Pre-flooded Cavity. Part 1: COOLAP-3 Code Development

Juwook Lee, Joongoo Jeon, Seokwon Whang, Hyun Sun Park*
Department of Nuclear Engineering, Seoul National University,
1 Gwanak-ro, Gwanak-gu, Seoul 08826, Republic of Korea
*Corresponding author: hejsunny@snu.ac.kr

1. Introduction

For the mitigation of severe accident in NPPs (Nuclear Power Plants), especially with respect to late containment failure, ex-vessel molten core coolability is of importance due to the risk associated with MCCI and containment over-pressurization.

As mitigation strategies for ex-vessel corium cooling in LWRs (Light Water Reactors), there are two strategies [1], a top-flooding strategy to fill the reactor cavity after the RV (Reactor Vessel) failure and a pre-flooding strategy to fill the cavity before RV failure. Typically, PWRs (Pressurized Water Reactors) in France and Germany adopt a top-flooding strategy. However, in Korea, a pre-flooding strategy has been considered. In the case of the pre-flooding strategy, the molten core released after the RV failure interacts with the water in cavity, accompanied by phenomena such as jet fragmentation and breakup, and the relocation of the molten core into the cavity bottom.

Many experiments such as FARO, KROTOS, and DEFOR were performed to the ex-vessel phenomena in the pre-flooded cavity. From the investigation of the experiments, various of physical and empirical models describing the phenomena related to FCI (Fuel-Coolant Interaction) were developed and validated. However, the initial conditions at the time of RV failure in the actual NPPs are uncertain, and also uncertainty exists in the models which describe phenomena. In order to evaluate the coolability of molten core in the pre-flooded cavity, it must reflect the uncertainty of accident scenario and the uncertainty of the model.

For that reason, COOLAP-2, a parametric code for evaluation of the ex-vessel coolability has been developed by Moriyama et al. [2] showing good agreement with FARO L-14, L-28, and L-31. Recently, further development of the code has been come out, COOLAP-3. Debris bed development and realistic particle size distribution models have been added, and number of model parameters were improved.

In this study, a sensitivity analysis was performed on each of COOLAP-2 and COOLAP-3 to evaluate the effect of two models on ex-vessel molten core coolability.

2. Development of COOLAP-3

In COOLAP-3, a particle size distribution model and a debris bed development model were added to COOLAP-2. The section 2.1 describes modeling concept of COOLAP-3, and the section 2.2 analytically discusses the effect of each two models on coolability with respect to DHF (Dry-out Heat Flux).

2.1. Modeling concept of COOLAP-3

COOLAP-3 was developed focusing on the cooling of molten core in pre-flooded cavity. It simulates a situation in which the molten core discharged from the RV is relocated to the bottom of cavity and cooling of relocated molten core is performed in pre-flooded cavity. Fig. 1 shows the behavior of the molten core in the cavity. The molten core jet discharged from the RV is accelerated by gravity and penetrates into the water pool.

By interaction with the water, the jet breakup takes place with fragmentation. In the case of an incomplete jet breakup, as shown in Fig. 1, the remaining part of jet after fragmentation and the particles which are not sufficiently cooled are relocated to cavity bottom as a cake which has a single lumped structure. And the sufficiently cooled particles are relocated to cavity bottom as a debris bed which has a porous internal structure which is composed of individual particles.

Heat transfer from the molten core to the water pool is divided into three types as shown in Fig. 2. The first is

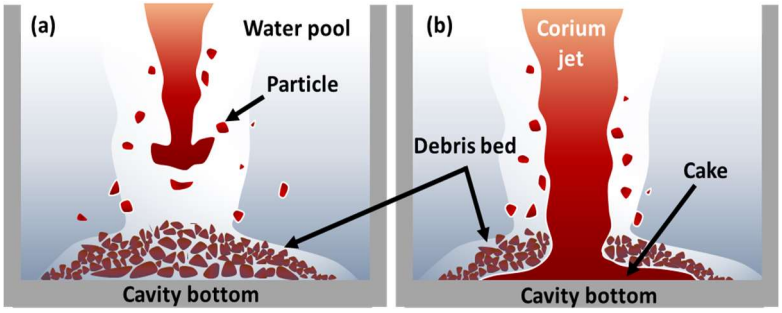

Fig. 1. Behavior of molten core in water pool: (a) complete jet breakup, (b) incomplete jet breakup

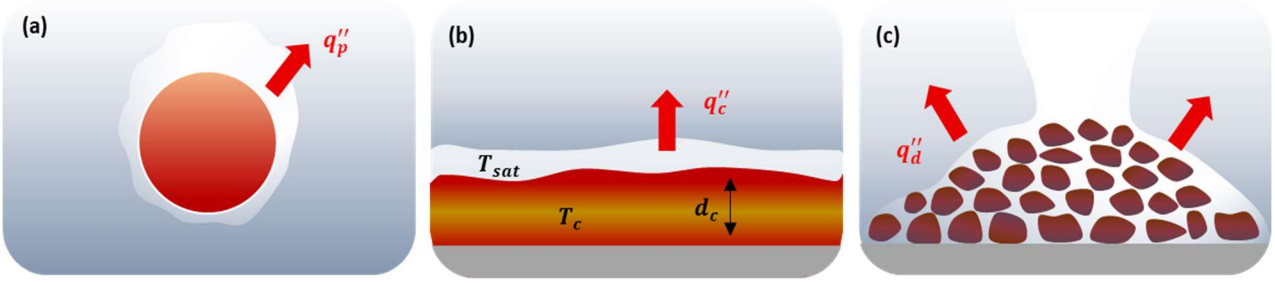

Fig. 2. Schematic diagram for ex-vessel molten core heat transfer: (a) particle, (b) cake, (c) debris bed

the heat transfer from particle to water that occurs during the sedimentation. The released heat from particle is calculated from the heat transfer correlations in accordance with the boiling regime. The second is the heat transfer from the cake to the water pool above it, and simple 1-dimensional equation is used for this type of heat transfer. The last one is the heat transfer from debris bed to water, and it is also calculated from the correlations which are same with that of the particle case. The detail is well described in the reference [2].

In the case of heat transfer from the high temperature debris bed to the water pool, inflow of water is limited by the steam outflow. For that reason, dry-out must be considered. To reflect this phenomenon, heat transfer from debris bed is limited by the DHF in COOLAP-3.

COOLAP-3 contains additional two models which describe key phenomena related to the ex-vessel coolability. The first model is Truncated Rosin-Rammer distribution [3] in which the minimum diameter is introduced into the size distribution of the particles as shown in Eq. (1). The minimum diameter was introduced to describe the phenomenon in which small particles in the debris bed are fluidized by steam flow and rearranged.

$$F(D_p) = 1 - exp\left(-\frac{D_p^n - D_{min}^n}{D_e^n}\right), D_p > D_{min} \quad (1)$$

The second is a debris bed development model developed based on the data of the DAVINCI experiment [4]. It considers the kinetic energy flux of sinking particles and it of upward steam flow. Model assumes a conical shape of debris bed. The radius and side slope angle of the debris bed are defined as shown in Eq. (2) and (3).

$$R = 0.615\left[\left(\frac{\Delta\rho^2}{\rho_p\rho_v\Delta h_{fg}}\right)\left(\frac{q_d'''H_s^2\tau}{\dot{m}}\right)\left(\frac{\alpha v_b D_{pc}^4}{(1-\varepsilon)v_p^4}\right)\right]^{1/3} \quad (2)$$

$$tan\theta = 4.127[(\frac{\rho_v\Delta h_{fg}}{\Delta\rho^2})(\frac{\dot{m}^2}{q_d'''H_s^2})(\frac{v_p^4}{\alpha v_b D_{pc}^4})] \quad (3)$$

2.2. Analysis of model effect on DHF

In the reactor scale, dry-out is the most important mechanism in ex-vessel coolability because initial temperature of debris bed and cake is much higher than the saturation temperature of the water pool. The equations of Lipinski type 1-dimensional DHF model [5] in COOLAP are as follows.

$$j_v = \frac{q_{dhf}''}{\rho_v h_{fg}} \quad (4)$$

$$j_l = w_r - \frac{q_{dhf}''}{\rho_v h_{fg}} \quad (5)$$

$$\frac{dP_v}{dz} = -\rho_v g - \frac{\mu_v}{K_{r.v}K}j_v - \frac{\rho_v}{\eta_{r.v}\eta}|j_v|j_v - \frac{F_i}{\varepsilon\alpha} \quad (6)$$

$$\frac{dP_l}{dz} = -\rho_l g - \frac{\mu_l}{K_{r.l}K}j_l - \frac{\rho_l}{\eta_{r.l}\eta}|j_l|j_l + \frac{F_i}{\varepsilon(1-\alpha)} \quad (7)$$

The absolute permeability and the absolute passability described in Eq. (6) and (7) are defined as a function of particle diameter as shown in Eq. (8) and (9) according to the Ergun equation. DHF becomes large as the SMD (Sauter Mean Diameter) of debris bed increases by increased permeability and passability. Because Truncated Rosin-Rammler distribution presents minimum diameter limitation, the increment of SMD in debris bed is accompanied by application of this model. Therefore, it can be expected that DHF will be increased by introducing Truncated Rosin-Rammler distribution.

$$K = \frac{\varepsilon^3 D_p^2}{150(1-\varepsilon)^2} \quad (8)$$

$$\eta = \frac{\varepsilon^3 D_p}{1.75(1-\varepsilon)} \quad (9)$$

The total heat release rate from DHF in the debris bed (Eq. (10)) is calculated by multiplying the cavity bottom area occupied by debris bed. It can be expected that the total heat release rate of the debris bed will vary significantly depending on the radius of the debris bed determined by Eq. (2).

$$\dot{q}_{dhf} = \sum_{i=1}^{n}[(q_{dhf.i}'' - q_c'') * A_{b.i}] \quad (10)$$

3. Sensitivity analysis

The sensitivity analysis was performed by using COOLAP-2 and COOLAP-3 to quantitatively compare the differences between the two versions of COOLAP. The section 3.1 describes the input data of the code, and the section 3.2 discusses the analysis results.

3.1. Input data

The analysis was performed with the plant condition like OPR-1000 for 1 hour, and the details of input data

are shown in Table 1. The total mass of the molten core relocated to cavity was assumed to be 99 tons, which is about 70% of the total fuel mass, and the initial containment pressure was assumed to be 0.12 MPa and the temperature of the cavity water was assumed to be 320 K. The free volume of containment, cavity bottom area, and normal operational power were determined by the design of plant.

Table 1: Input data for sensitivity analysis

Input parameter	Value
Molten core mass, ton	99
Initial containment pressure, MPa	0.12
Initial cavity water temperature, K	320
Initial molten core temperature, K	2800
Containment free volume, m3	78395
Cavity bottom area, m2	67.6
Normal operational power, MWth	2815

3.2. Analysis results and discussion

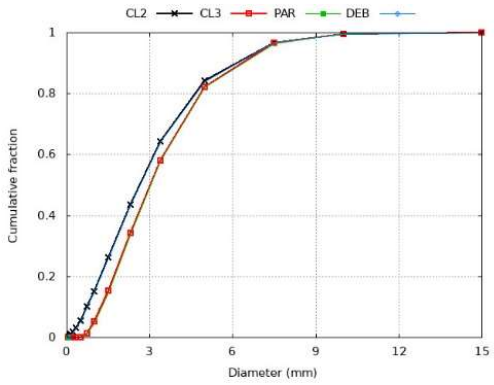

Fig. 3. Cumulative mass fraction according to diameter

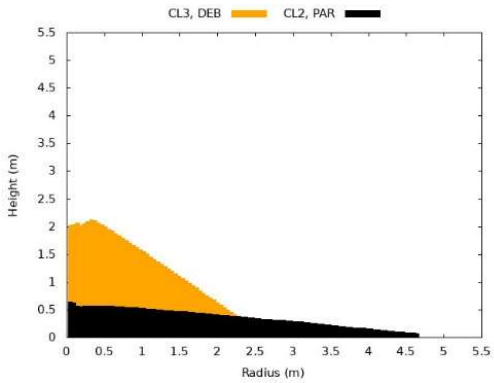

Fig. 4. Shape of debris bed (half)

CL2 and CL3 represent the results from COOLAP-2 and COOLAP-3, respectively. In order to analyze the effect of individual models, the results from the code only with Truncated Rosin-Rammler distribution model and the results from the code only with the debris bed development model are included, and the legends are PAR and DEB, respectively.

Fig. 3 and Fig. 4 show the direct effect of each model. For CL2 and DEB, there is Rosin-Rammler distribution as a particle size distribution. From the application of Truncated Rosin-Rammler distribution in CL3 and PAR, they show increase in SMD almost 1.73 times compared to CL2 and DEB, and the calculated minimum diameter of particle in these cases is about 0.5mm.

For CL2 and PAR, there is 10 degrees of the repose angle for debris bed development. From this repose angle, as shown in Fig.4, a flat debris bed with a radius about 4.6m was formed. On the other hand, CL3 and DEB where debris bed development model is applied show conical shape with 2.6m in radius and 2m in height.

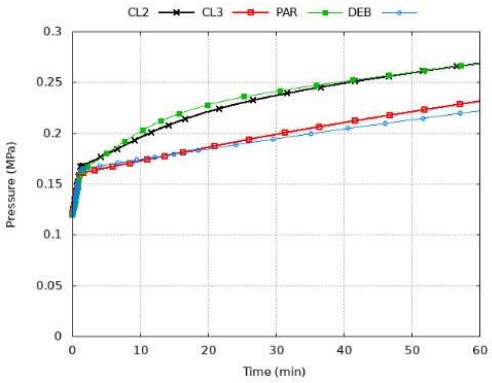

Fig. 5. Containment pressure history

Fig. 5 shows the containment pressure history for 1 hour. Because the only reason of pressure increase in code calculation is the generation of steam due to cooling of molten core, the tendency difference of containment pressure increase can be explained by the coolability of molten core. During the particle sedimentation, containment pressure increase slows down slightly in CL3 and PAR due to degradation of heat transfer caused by increment of average particle size. This can be confirmed through the high initial temperature of the debris bed about CL3 and PAR, as shown in Fig. 6.

After the sedimentation, CL3 and DEB show much slower increase in containment pressure. The reason of slower pressure increase is reduction of total heat release rate in debris bed. As shown in Fig. 4, Debris bed in CL3 and DEB occupies much smaller area than it of CL2 and PAR. It means that the total heat release rate defined in Eq. (10) is smaller in CL3 and DEB than CL2 and PAR. From that reason, as shown in Fig. 6, coolability of debris bed is much degraded in CL3 and DEB, resulting in a delay in the pressure increase. Also, in Fig. 6, there is difference about coolability between CL3 and DEB. This difference comes from the increment of permeability and passability caused by minimum diameter of Truncated Rosin-Rammler distribution. Because of large SMD in CL3, DHF is increased and the coolability is improved accordingly. For the same reason, CL2 and PAR show similar difference in coolability.

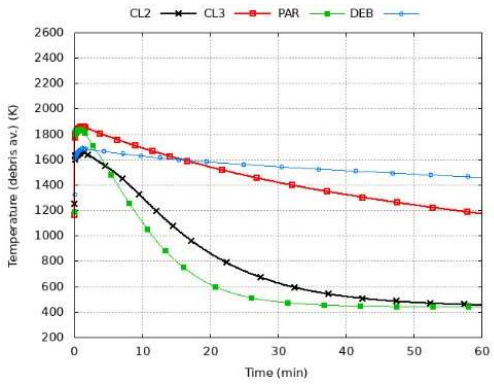

Fig. 6. Debris bed temperature history

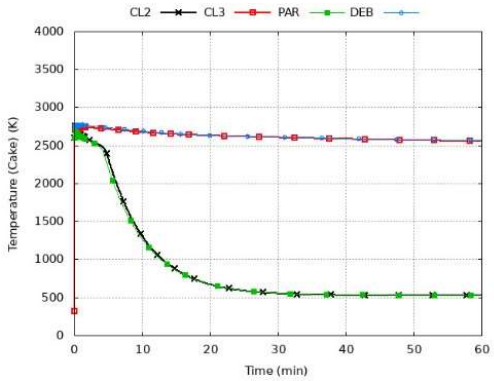

Fig. 7. Cake temperature history

Fig. 7 shows cake temperature history. CL3 and DEB show much degradation in coolability of cake. The coolability of cake is dependent on thickness of cake because its heat flux is calculated inversely proportional to thickness. From this reason, total mass and radius of cake directly effect on coolability of cake. As shown in Fig. 8, although there is slight difference in cake mass, it is negligible. Then, the radius determined by the debris bed development model can be said to be the most dominant cause of difference.

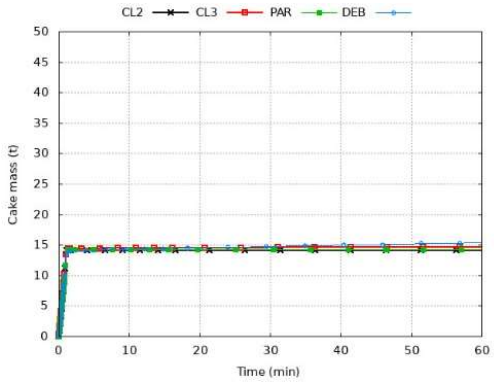

Fig. 8. Cake mass history for

4. Conclusions

In this study, COOLAP-3 including models for key phenomena which are highly related to coolability was developed.

COOLAP-3 includes Truncated Rosin-Rammler distribution, which reflects the fluidization of small particles in the debris bed and a debris bed development model, which considers the kinetic energy flux of sinking particles and the upward flow of steam. By additional two models, it is possible to reflect the physical phenomena, which are most important in ex-vessel coolability.

Sensitivity analysis according to each model was performed using COOLAP-2 and COOLAP-3. The effect of each model in coolability can be explained by DHF. For the Truncated Rosin-Rammer distribution, the coolability is improved by the increment of absolute permeability and absolute passability. On the other hand, the debris bed development model causes a decrease in the cross-sectional area where dry-out occurs, resulting in a degradation of coolability.

ACKNOWLEDGEMENT

This work was supported by the Nuclear Safety Research Program through the Korea Foundation of Nuclear Safety (KoFONS) using the financial resource granted by the Nuclear Safety and Security Commission (NSSC) of the Republic of Korea (Grant No. 2106033-0222-CG100).

REFERENCES

[1] B. R. Sehgal, ed. *Nuclear safety in light water reactors: severe accident phenomenology*. Academic Press, pp. 307-345, 2011.
[2] K. Moriyama, et al. "Parametric Model for Ex-Vessel Melt Jet Breakup and Debris Bed Cooling." *International Conference on Nuclear Engineering*.
Vol. 51517. American Society of Mechanical Engineers, 2018.
[3] W. Jung, et al. "Minimum diameter limit of particle size distribution and its effect on coolability of debris bed." *Nuclear Engineering and Design* 363 (2020): 110606.
[4] E. Kim, et al. "Development of an ex-vessel corium debris bed with two-phase natural convection in a flooded cavity." *Nuclear Engineering and Design* 298 (2016): 240-254.
[5] R. J. Lipinski, *Model for boiling and dryout in particle beds*. No. NUREG/CR--2646. Sandia National Labs., 1982.